

Mass spectral analysis and quantification of Secondary Ion Mass Spectrometry data

A. K. Balamurugan, S. Dash and A. K. Tyagi
Materials Science Group, Indira Gandhi Centre for Atomic Research
Kalpakkam 603102, India.

Abstract

This work highlights the possibility of improving the quantification aspect of Cs-complex ions in SIMS (Secondary Ion Mass Spectrometry), by combining the intensities of all possible Cs-complexes. Identification of all possible Cs-complexes requires quantitative analysis of mass spectrum from the material of interest. The important steps of this mass spectral analysis include constructing fingerprint mass spectra of the constituent species from the table of isotopic abundances of elements, constructing the system(s) of linear equations to get the intensities of those species, solving them, evaluating the solutions and employing a regularization process when required. These steps are comprehensively described and the results of their application on a SIMS mass spectrum obtained from D9 steel are presented. It is demonstrated that results from the summation procedure, which covers entire range of sputtered clusters, is superior to results from single Cs-complex per element. The result of employing a regularization process in solving a mass spectrum from an SS316LN steel specimen is provided to demonstrate the necessity of regularization.

1 Introduction

Knowledge of chemical composition is an important aspect in the study of materials. As a surface analytical technique, Secondary Ion Mass Spectrometry (SIMS), is employed for composition profiling of materials in widely varying fields like semiconductor industry[1] and nuclear technology[2, 3]. This technique has high sensitivity, surface specificity, and high dynamic range. However, it lacks quantification because of the dependence of yield of secondary ions on the composition (matrix) of the surface from which it is ejected.[4, 5] This artefact of the technique is called as matrix effect. In semiconductor industry, the number of commonly analyzed semiconductor materials is limited. Hence, semiconductor research uses matrix-matched standards to quantify SIMS measurements.[6] However, in a general case, like a compound multilayer or an alloy with oxidized surface, the composition is likely to vary over a vast range in the volume analyzed. Such specimens would require a very large number of standards matching each of those compositions to quantify the data. Hence, employing matrix-matched standards in such cases is near to impossible. The matrix effect in the intensities of XC_n^+ secondary ions measured with Cs^+ primary ions (where X stands for an atom from the specimen and n is equal to 1 or 2) was shown by Gao [7, 8] to be much lower (in some cases, even by orders of magnitude) than that in secondary elemental ions. However, there is considerable deviation of the composition computed from these XC_n signals from the actual composition. In

spite of developments in understanding the formation process of these species (for example, ref [9–17]), a gap remains in this approach in reaching complete quantification. The current work provides an incremental step in filling this gap.

2 Theory

The XC_s^+ secondary ions are understood to be formed by the combination of a resputtered Cs^+ ion with a sputtered neutral atom from the specimen [9–17]. Since secondary neutrals are formed as different atomic clusters[17–20], the intensities of the Cs complexes of all these clusters should be combined to enhance the quantitateness of XCs SIMS. This was earlier verified with a limited number of Cs complexes [21]. However, testing this with all the Cs complexes involves quantitative measurement of the intensities of the species constituting a mass spectrum and then computing the composition from those intensities.

3 Material and Methods

In this report, the details of this process are presented by analyzing a mass spectrum obtained from a sample of D9 steel, produced by M/s. Valinox, France. D9 is the steel used in fast reactors as a construction material of core components because of its resistance to void swelling.[3] It was selected as a material for test in this report, because it is a multi-component alloy with known composition. The implementation of the above theory involves setting up and solving systems of linear equations to know the composition of the mass spectrum. A mass spectrum is analyzed completely by considering its peaks one after another. With a peak chosen for analysis, a probable species with its mono-isotopic mass equal to the mass of that peak is first identified. This species could be mono atomic or a poly atomic cluster. Its fingerprint mass spectrum has to be constructed and matched with the experimental mass spectrum. If this species contains n number of elements, the number N of different isotopic combinations forming this species is given by

$$N = \prod_{i=1}^n \frac{(r_i + s_i - 1)!}{r_i!(s_i - 1)!} \quad (1)$$

where r_i , is the number of atoms of the i^{th} element in the species and s_i is the number of isotopes of the i^{th} element. Those isotopic combinations with differences in mass, which are not discernible by the resolving power of the mass analyzer, appear as a single peak in the mass spectrum. (For example, in the cluster species CrFe, the combinations, $^{54}\text{Cr}^{54}\text{Fe}$ and $^{52}\text{Cr}^{56}\text{Fe}$ differ by a mass of 0.003u. A typical mass spectrometer with mass resolving power (MRP) of 500 cannot resolve these two combinations since the MRP required to resolve these species is 35428.) Hence, generally in a mass spectrum, the number of peaks corresponding to a cluster species is fewer than N . This group of peaks from the mass spectrometer forms the fingerprint spectrum of the species after normalizing the sum of their intensities to unity.

The fingerprint spectra of many species are likely to overlap with each other. The difficulty of identifying and measuring the intensities of such species in the measured spectrum depends on the number and complexity of their fingerprint spectra. The overlapping fingerprint spectra in the measured spectrum are mathematically represented by a system of linear equations. This system of equations contains one equation for every peak in the spectrum that is the resultant of overlap.

For q number of species, overlapping with each other, constituting p number of peaks, the system of equations is

$$\sum_{j=1}^q a_{ij} s_j + \delta_i = m_i \quad (2)$$

where i runs from 1 to p representing the p number of equations and m_i is the measured intensity of the i^{th} peak. s_j is the intensity of the j^{th} species, to be solved for. If the fingerprint mass spectrum of the j^{th} species has a peak at the mass of the i^{th} peak, a_{ij} is the intensity of that peak of the fingerprint mass spectrum. Otherwise, a_{ij} is zero. δ_i is the noise that occurred while measuring m_i , which is not known. This term was added for completeness of mathematical description. However, the above set of equations has to be solved without the knowledge of this term. The above set of equations can be represented in matrix form, after neglecting the noise term as,

$$\mathbf{A} \mathbf{s} = \mathbf{m} \quad (3)$$

where \mathbf{A} is the $p \times q$ matrix containing the elements a_{ij} of eqn.2. \mathbf{s} is the $q \times 1$ solution vector and \mathbf{m} is the $p \times 1$ input vector containing s_j and m_i of eqn.2 as their elements respectively. The solution providing the least squared deviation between the L.H.S. and R.H.S. of the above equation is obtained by solving the normal form of the above equation,

$$\mathbf{A}^T \mathbf{A} \mathbf{s} = \mathbf{A}^T \mathbf{m} \quad (4)$$

where $\mathbf{A}^T \mathbf{A}$ is a $p \times p$ matrix and $\mathbf{A}^T \mathbf{m}$ is a $p \times 1$ vector. \mathbf{A}^T means transpose of \mathbf{A} .

In a few circumstances, the solution may turn out to be erroneous (including negative values for the intensities of a few species) due either to the intensity of noise or to wrong choice of species or both. If the error in the solution is due to the noise in the data, the solution can be optimized by following a regularization algorithm such as the iterative algorithm discussed by Gautier *et al* [22, 23] to deconvolve instrumental broadening from SIMS depth profiles. The convolution matrix, solution of deconvolution and measured depth profile found in Ref. [22, 23] are to be replaced by the isotope abundance matrix \mathbf{A} , solution for intensities \mathbf{s} and the measured mass spectrum \mathbf{m} respectively to regularize the solution of eqn 3. Out of the two regularization conditions imposed in Ref. [22, 23], the condition of positivity has to be retained while rejecting the condition of smoothness since the intensities need not vary smoothly from species to species. If the choice of species is wrong, the intensities of one or more species in the solution may remain to be negative even after the regularization process. In such cases, other probable species have to be tried out and the process has to be repeated until all the correct species are identified.

The concentration of an element is computed as the fraction of the number of atoms of that element in the Cs complexes to the total number of atoms in all of the Cs complexes excluding atoms of Cs and any other element like O that might originate from the instrument,

$$c_i = \frac{\sum_{j=1}^m n_{ji} s_j}{\sum_{k=1}^n \sum_{l=1}^{e_k} n_{lk} s_k} \quad (5)$$

where c_i is the concentration of the i^{th} element, m is the number of species containing the i^{th} element, n_{ji} is the number of atoms of i^{th} element in the j^{th} such species, s_j is the intensity of that (j^{th}) species, n is the total number of species identified, e_k is the number of elements (excluding Cs and any other element as mentioned above) in the k^{th} species, n_{lk} is the number of atoms of the l^{th} element in the k^{th} species and s_k is the intensity of the k^{th} species.

The process of identifying and measuring the intensities of the species constituting a mass spectrum will be discussed here with a SIMS mass spectrum obtained from a D9 specimen. This mass spectrum was obtained using a SIMS (Cameca ims-4f) system by employing a 20 nA, 5.5 keV Cs^+ primary ion beam for sputtering the specimen. The primary ion beam was rastered over a square area of width 150 μm and the secondary ions were collected from the central circular area of diameter 33 μm . The mass spectrometer was operated with a mass resolving power of 500 and energy band-pass of 125 eV for the secondary ions. Eleven data points were recorded around each integral mass number to construct the peaks. A portion of the raw mass spectrum in addition to the peak values as calculated below is shown in figure 1.

4 Calculation

The SIMS mass spectral peaks have the shape of the convolution of the ion-beam crossover with the exit slit of the mass analyzer. The data required for analysis are the heights of these peaks. Since the data is subject to noise and the peaks have a sparse density of data, the highest raw data point of many of the peaks do not represent the apex position. Hence, the spectrum was smoothened by 3-point weighted average with the central point receiving a weight of 50% and the neighboring points a weight of 25%. After smoothening, the heights of the peaks decreased proportionately and almost all of the peaks obtained a unique apex point as shown in the figure. The apex values of most of the smoothened peaks could be considered as the heights of the respective peaks. The heights of the remaining peaks were estimated manually. The peak values so estimated are shown as a bar graph in figure 2.

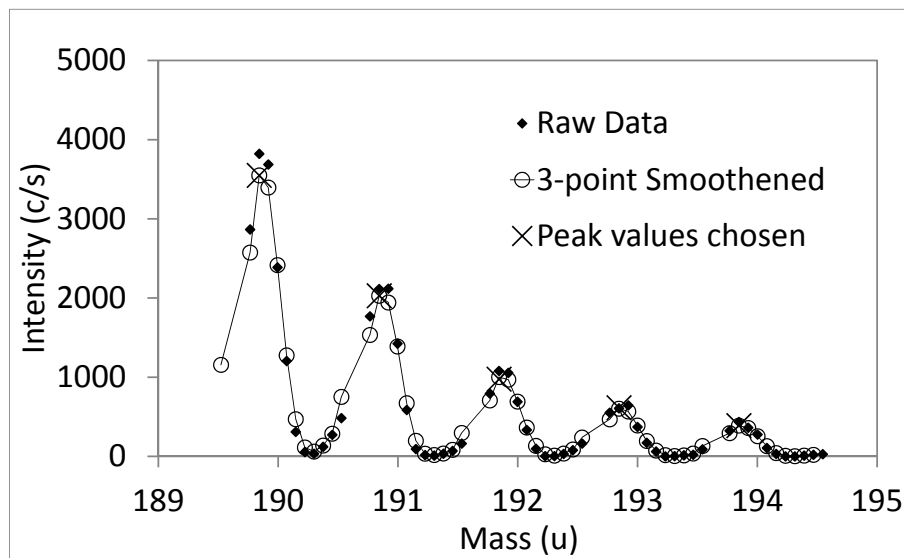


Figure 1: A portion of raw mass spectrum showing extraction of peak values

The two strongest peaks in this mass spectrum, at mass numbers 133u and 266u, are those of Cs and Cs_2 respectively. The next highest peak is at mass number, 189u that is the mass of $^{56}Fe^{133}Cs$.

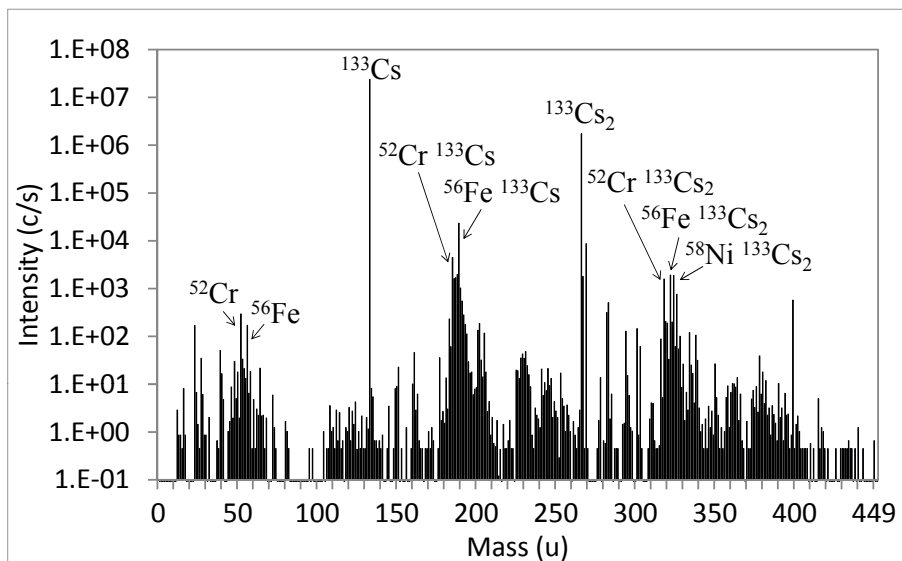


Figure 2: The mass spectrum over the complete mass range, constructed using the peak values picked up from the raw mass spectrum. The names of a few of the prominent species are labeled to the corresponding peaks.

Setting up and solving eqn.3 for FeCs alone results in a slightly higher estimate for the intensity of FeCs, to minimize the squared deviation from the measured intensity at mass number 187u that is the mass of $^{54}\text{Fe}^{133}\text{Cs}$ as well as that of $^{54}\text{Cr}^{133}\text{Cs}$. The higher estimate for FeCs compensates the absence of $^{54}\text{Cr}^{133}\text{Cs}$ in the equation for mass number 187u. After including CrCs in the equation, this error in the estimate for FeCs is corrected. In this manner, the probable species contributing to all the peaks can be tried out one after the other until all the peaks are successfully characterized. The final solution is not affected by the order in which the the peaks of the mass spectrum are chosen for analysis.

5 Results and Discussion

In the above mass spectrum, twenty four species were identified overlapping with each other spanning over the mass range from 177u to 208u, as shown in figure 3. In this figure, the measured spectrum is shown wider in the background and the constituent fingerprint spectra multiplied by their respective intensities are shown narrower in the foreground. With the perfect solution, the sum of the constituent spectra should be as equal to the measured spectrum as possible as shown in figure 3. The analysis of the complete mass spectrum resulted in identification of 165 species that are tabulated in Table 1. Most of them are Cs complexes that are required for the proposed quantification process.

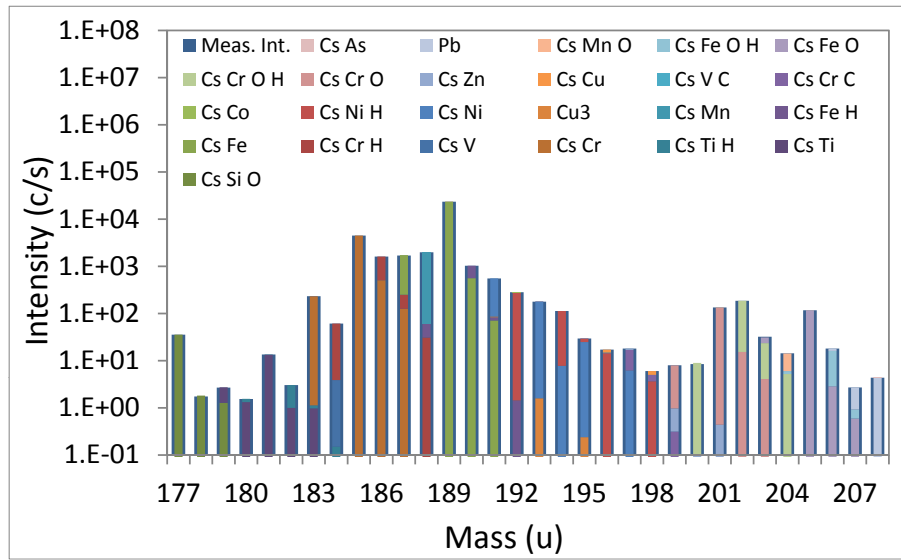


Figure 3: A portion of the complete mass spectrum shown in figure 2, labelled here as “Meas. MS”, and its composition computed using *eqn 4*

Species	Intensity (c/s)	Species	Int. (c/s)	Species	Int. (c/s)
Cs	23732613.0	Cr O H Cs ₂	13.70	Fe Ni O Cs ₂	3.17
Cs ₂	1745702.5	Fe Cr O Cs ₂	13.47	C	2.93
Fe Cs	25458.3	Mn	13.12	Cr Fe H Cs	2.86
Cr Cs	5328.6	Cr C Cs	12.86	Cr O ₂ H Cs ₂	2.78
Ni Cs ₂	2749.8	Mo O H Cs	10.41	Ti H Cs	2.77
Fe Cs ₂	2094.4	Al Cs	10.15	Ni O Cs ₂	2.77
Mn Cs	1919.7	Fe Cr Cs ₂	9.62	Fe Cr N	2.72
Cr Cs ₂	1892.2	Si H Cs ₂	9.58	Cu	2.64
H Cs ₂	1790.9	Cr Ni Cs	9.42	Fe H	2.58
Cr H Cs	1311.1	O H Cs	9.08	Zn Cs	2.34
Ni Cs	685.7	O ₃	8.35	V O Cs ₂	2.32
Cs ₃	574.3	H Cs	8.16	Al ₂	2.19
Fe H Cs	511.6	Mn O Cs	8.15	Fe ₂ O Cs	2.14
O H Cs ₂	507.7	O	8.14	Cr C N Cs ₂	2.01
Ni H Cs	402.5	Cu ₃	8.10	W Cs	2.00
Cr	352.8	O Cs	8.07	Fe O ₂ Cs	1.94
O Cs ₂	315.6	Pb	8.05	Fe ₂ O	1.82
Cr O H Cs	204.6	Ni C Cs ₂	8.01	Cr O ₂ Cs	1.81
Cl Cs ₂	197.4	Mo H Cs ₂	7.97	Mn O Cs ₂	1.80
Fe	186.2	Ni Cr Cs ₂	7.35	V	1.72
Na	169.3	Si	6.60	Cu ₂	1.54
Fe H Cs ₂	167.4	Fe ₂ O Cs ₂	6.54	Al Cs ₂	1.53
Cr O Cs	160.5	Co Cs	6.53	Cr O N Cs ₂	1.51
Mo Cs	155.1	Na ₂	6.46	O ₂	1.39
Cr O Cs ₂	144.1	Zn	6.44	Cr ₂	1.37
Si Cs ₂	139.6	Fe Ni Cs	5.72	Cr Mn O	1.29
Fe O Cs	128.1	Cs H ₂	5.41	Ni ₂ O Cs ₂	1.25
Fe O Cs ₂	114.2	Cr Fe O Cs	5.37	Na Cs	1.24
Mo H Cs	107.1	Fe Cr O	5.27	Fe Cu	1.24
Ni H Cs ₂	74.7	Fe Ni H Cs ₂	5.25	S Cs ₂	1.10
Ti C Cs ₂	63.8	F Cs ₂	5.22	O H ₂ Cs ₂	0.99
Mo Cs ₂	59.1	Co Cs ₂	5.07	P Cs ₂	0.94
K	54.8	Fe ₂ H Cs ₂	5.02	O H	0.87
Si Cs	49.9	Cr ₂ Cs	5.00	N	0.87
Fe ₂ Cs ₂	43.2	Fe Cr	4.70	As Cs ₂	0.86
Si O Cs	38.8	Ti H	4.61	C H	0.85
Al	35.1	Ni ₂ Cs ₂	4.57	Fe C	0.82
Mo O Cs	32.4	Cr ₂ O Cs ₂	4.45	Co ₂	0.81
Cr O ₂ Cs ₂	32.0	Si O Cs ₂	4.42	Mn ₂	0.77
Fe O H Cs ₂	31.6	Cr ₂ C Cs ₂	4.35	Fe ₂ H	0.69
Cr H Cs ₂	31.1	Fe ₂ H Cs	4.24	Si H ₂	0.69
Ti	28.9	Cr O C Cs ₂	4.16	Mn O ₂ Cs	0.66
Fe Ni Cs ₂	26.5	Si O H Cs ₂	4.14	P Cs	0.66
Ni	25.4	Cr ₂ O	4.08	S	0.66
Cr ₂ O Cs	24.7	V Cs ₂	3.89	Si H	0.61
Mn Cs ₂	22.9	Ni Cr O Cs ₂	3.86	V O ₂ Cs ₂	0.60
H ₂ O Cs	22.8	Fe Ni	3.75	S Cs	0.48
Cr C	22.1	V Cs	3.73	Na Cs ₂	0.45
Cr Fe Cs	20.3	Cu Cr O	3.63	V ₃	0.41
Al ₂ Cs ₂	20.1	C Cs	3.52	V C Cs	0.35
Ti Cs	18.1	V C Cs ₂	3.50	Sn Cs	0.26
Ca	17.1	Cu Cs ₂	3.35	Co	0.20
Fe O H Cs	14.5	Cu Cs	3.34	Ni H	0.17
Fe ₂ Cs	13.9	Fe ₂	3.27	As Cs	0.06
C Cs ₂	13.9	Nb Cs	3.17	Nb Cs ₂	0.06

Table 1: Species identified as constituents of the complete mass spectrum shown in figure 2

Element	Concentration from			
	Known	Multi Cs-species	Single Cs-species	Atomic sec. ions
Fe	65.22	64.034	71.088	27.761
Cr	16.04 \pm 0.53	20.684	14.877	52.593
Ni	13.27 \pm 0.47	8.896	7.678	3.786
Mn	1.92 \pm 0.051	4.348	5.360	1.955
Si	1.49 \pm 0.099	0.548	0.390	0.984
Mo	1.28 \pm 0.029	0.828	0.433	0.000
Ti	0.29 \pm 0.006	0.188	0.050	4.314
C	0.17 \pm 0.023	0.258	0.039	0.437
Al	< 0.10	0.115	0.028	5.231
V	0.049 \pm 0.003	0.031	0.010	0.257
Cu	< 0.044	0.016	0.011	0.393
As	< 0.025	0.002	0.000	0.000
P	< 0.025	0.004	0.003	0.000
Co	0.019 \pm 0.005	0.026	0.014	0.030
Pb	< 0.019	0.000	0.000	1.200
W	< 0.017	0.004	0.006	0.000
Nb	< 0.010	0.007	0.009	0.000
S	< 0.009	0.004	0.003	0.098
Sn	< 0.003	0.001	0.001	0.000
Zn	-	0.005	0.007	0.960

Table 2: Comparison of estimates of composition arrived using different methods with the known composition of D9

Composition of D9 computed from Table 1 using eqn. 5 is shown in Table 2 in the column named ‘Multi-species’. The standard composition of D9 is titled as ‘Known’, the composition computed using one Cs complex per element is titled as ‘Single-species’ and the composition computed using atomic secondary ions like Fe^+ and Cr^+ is titled as ‘Atomic sec. ions’. The estimate of composition using single Cs-complex per element shows drastic improvement from the estimate obtained by using atomic secondary ions. This improvement is further enhanced by combining Cs complexes. The estimation of the concentration of Fe is very close to the actual concentration and that of Cr exceeds the actual value, while those of most of the other elements show a tendency to approach the actual concentration. The formation of Cs complexes is influenced by different parameters. For example, the intensity of an XC species, where X is an atom of a compound semiconductor or a dopant in Si, is shown to depend on polarizability of X.[12] Similar are the results in the case of steel, discussed here. The ratios, intensity of Cs complex to concentration, I_{XC_s}/C_X , of Ni, Cr, Fe and Mn, normalized to the ratio of Fe are, 0.137, 0.852, 1 and 2.52 respectively. This is in considerable accordance with Ref [12]. The formation of an XC₂ species is influenced by the electron affinity of X [8]. The similar ratios, I_{XC_s2}/C_X for the above four elements are respectively, 6.46, 3.67, 1 and 0.371. Thus, the disproportionalities caused by the formation of XC are countered to some extent

Species	Solution		Species	Solution	
	LSD	Regul.		LSD	Regul.
O Cs ₂	62907	62907	C ₂ Cs ₂	-702	785
Cl Cs ₂	35628	35628	O ₂ H Cs ₂	585	585
Si Cs ₂	32663	35397	Al Cs ₂	283383	480
F Cs ₂	20715	20715	F H ₂ Cs ₂	417	420
O ₂ Cs ₂	20658	20664	Na Cs ₂	305	388
O H Cs ₂	20460	20460	O H ₂ Cs ₂	339	340
C ₂ H Cs ₂	46307724	3110	F H Cs ₂	222	226
C ₂ H ₂ Cs ₂	-988227	2998	Cl H Cs ₂	141	141
P Cs ₂	2139	2179	Cr ₅ O ₂	25865	38
O ₂ H ₂ Cs ₂	844	844	Mn ₂ O ₃ Cs	-45615716	5
Fe ₅ C	-5775	805			

Table 3: The least squared deviation (LSD) and regularized (“Regul.”) solutions for a group of species from an SS316LN sample kept at 550°C for 30,000 hours

by the formation of XC_{s2}. This is overdone in the case of Cr resulting in a net higher estimate for its concentration. In general, combining all the species of the form XC_{s_n}, where X is any cluster, is found to take the estimate for composition towards the actual one.

As an example showing the inevitability of the regularization process, the least squared deviation and the regularized solutions for the intensities of a group of species ejected from the surface of an SS316LN sample kept at 550°C for 30,000 hours, is shown in Table 3. This regularized solution was reached through 27 steps of the iterative regularization process discussed in section 3. This is an example showing how weird the initial solution could be and the capability of the regularization process to arrive at a meaningful solution. However, it should be remembered that in addition to mathematical rigor, physical reasoning should also be followed in the choice of species for analysis.

6 Conclusion

The technique of combining all XC_{s_n} complexes (where X is any cluster) to compute composition is verified to advance the current status of quantification with Cs complexes a step further towards better quantification by two means. One is by the inclusion of atoms in the left out Cs complexes. The other is by the tendency of the disproportionalities of the intensities of XCs and XC_{s2} species to the concentration of X to counter each other. Delineation of species constituting a mass spectrum, which is a prerequisite for this quantification technique, is aided by the mass spectral analysis described here.

The authors thank Dr. R. Ramaseshan for his help in proof reading and valuable suggestions.

References

- [1] Takayuki Aoyama, Hiroko Tashiro, and Kunihiro Suzuki, J. Electrochem. Soc. **146** (5), 1879 (1999).

- [2] N. Sivai Bharasi, K. Thyagarajan, H. Shaikh, M. Radhika, A.K. Balamurugan, S. Venugopal, A. Moitra, S. Kalavathy, S. Chandramouli, A.K. Tyagi, R.K. Dayal, and K.K. Rajan, *Metalurgical and Materials Transactions A* **43**, 561 (2012).
- [3] C. David, B.K. Panigrahi, S. Balaji, A.K. Balamurugan, K.G.M. Nair, G. Amarendra, C.S. Sundar, Baldev Raj, *Journal of Nuclear Materials* **383**, 132 (2008).
- [4] V. R. Deline, William Katz, C. A. Evans Jr., Peter Williams, *Appl. Phys. Lett.* **33**, 832 (1978).
- [5] Ming L. Yu, Wilhad Reuter, *J. Vac. Sci. Technol.* **17**, 36 (1980).
- [6] D. P. Leta, G. H. Morrison, *Anal. Chem.* **52** (3), 514 (1980).
- [7] Y. Gao, *J. Appl. Phys.* **64**, 3760 (1988).
- [8] Y. Gao, Y. Marie, F. Saldi, H.N. Migeon, *Proceedings of the 9th International Conference on Secondary Ion Mass Spectrometry - SIMS-IX*, Yokohama, Japan, 7-12 November, 406 (1993).
- [9] Charles W. Magee, William L. Harrington, Ephraim M. Botnick, *International Journal of Mass Spectrometry and Ion Processes* **103**, 45 (1990).
- [10] H. Gnaser, *International Journal of Mass Spectrometry and Ion Processes* **174** 119 (1998)
- [11] Howard E. Smith, Bang-Hung Tsao, James Scofield, *Materials Science Forum* **527-529**, 629 (2006).
- [12] H. Gnaser, H. Oechsner, *Surface Science Letters* **302**, L289 (1994).
- [13] T. Mootz, F. Adams, *International Journal of Mass Spectrometry and Ion Processes* **152** 209 (1996).
- [14] K. Wittmaack *Nuclear Instruments and Methods in Physics Research B* **64**, 621 (1992).
- [15] T. Wirtz, H.-N. Migeon, H. Scherrer, *International Journal of Mass Spectrometry* **225**, 135 (2003).
- [16] Yu. Kudriavtsev, A. villegas, A. Godines, R. Asomoza. *Appl. Surf. Sci.* **206**, 187 (2003).
- [17] N. Mine, B. Douhard, L. Houssiau, *Applied Surface Science* **255**, 973 (2008).
- [18] J. Goschnick, M. Fichtner, M. Lipp, J. Schuricht, H.J. Ache, *Applied Surface Science* **70/71**, 63 (1993).
- [19] T. Welzel, S. Mandl, K. Ellmer, *J. Phys. D: Appl. Phys.* **47**, 065204 (2014).
- [20] S.F. Belykh, V.I. Matveev, I.V. Veryovkin, A. Adriaens, F. Adams, *Nuclear Instruments and Methods in Physics Research B* **155**, 409 (1999).
- [21] A.K. Balamurugan, S. Rajagopalan, S. Dash, A.K. Tyagi, *Proceedings of the 23rd International Conference on Surface Modification Technologies - SMT-XXIII*, Mamallapuram, India, November, 537 (2009)
- [22] B. Gautier, R. Prost, G. Prudon, J. C. Dupuy, *Surface and Interface Analysis*, **24** 733 (1996).
- [23] B. Gautier, J. C. Dupuy, R. Prost, G. Prudon, *Surface and Interface Analysis*, **25**, 464 (1997).